

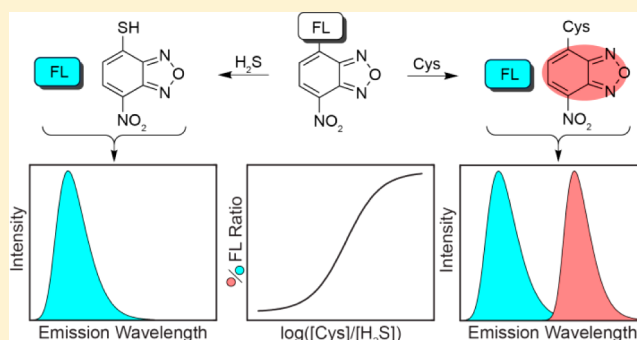
# Ratiometric Measurement of Hydrogen Sulfide and Cysteine/Homocysteine Ratios Using a Dual-Fluorophore Fragmentation Strategy

Matthew D. Hammers and Michael D. Pluth\*

Department of Chemistry and Biochemistry, Institute of Molecular Biology, Material Science Institute, 1253 University of Oregon, Eugene, Oregon 97403, United States

## S Supporting Information

**ABSTRACT:** Hydrogen sulfide ( $\text{H}_2\text{S}$ ) is an integral signaling molecule in biology with complex generation, translocation, and metabolism processes that are intertwined with cellular thiols. Differentiating the complex interplay between  $\text{H}_2\text{S}$  and biological thiols, however, remains challenging due to the difficulty of monitoring  $\text{H}_2\text{S}$  and thiol levels simultaneously in complex redox environments. As a step toward unraveling the complexities of  $\text{H}_2\text{S}$  and thiols in sulfur redox homeostasis, we present a dual-fluorophore fragmentation strategy that allows for the ratiometric determination of relative  $\text{H}_2\text{S}$  and cysteine (Cys) or homocysteine (Hcy) concentrations, two important metabolites in  $\text{H}_2\text{S}$  biosynthesis. The key design principle is based on a nitrobenzofurazan-coumarin (NBD-Coum) construct, which fragments into spectroscopically differentiable products upon nucleophilic aromatic substitution with either  $\text{H}_2\text{S}$  or Cys/Hcy. Measurement of the ratio of fluorescence intensities from coumarin and the NBD-Cys or NBD-Hcy adducts generates a sigmoidal response with a dynamic range of 3 orders of magnitude. The developed scaffold displays a rapid response ( $<1$  min) and is selective for sulfhydryl-containing nucleophiles over other reactive sulfur, oxygen, and nitrogen species, including alcohol- and amine-functionalized amino acids, polyatomic anionic sulfur species, NO, and HNO. Additionally, NBD-Coum is demonstrated to differentiate and report on different oxidative stress stimuli in simulated sulfur pools containing  $\text{H}_2\text{S}$ , Cys, and cystine.



Hydrogen sulfide ( $\text{H}_2\text{S}$ ) has emerged as an integral biological signaling molecule since its discovery as the third gas transmitter.<sup>1–5</sup> Produced endogenously from cysteine (Cys), homocysteine (Hcy), and cystathionine, enzymatic  $\text{H}_2\text{S}$  biosynthesis occurs primarily from cystathionine- $\beta$ -synthase (CBS) in the brain, cystathionine- $\gamma$ -lyase (CSE) in the liver and kidneys, and 3-mercaptopyruvate sulfurtransferase (3-MST) in mitochondria. Once produced,  $\text{H}_2\text{S}$  exerts important effects on vasorelaxation, inflammation, cell angiogenesis, hippocampal memory formation, and hepatic circulation.<sup>1,6–11</sup> Additionally, abnormal  $\text{H}_2\text{S}$  levels are implicated in central nervous system diseases such as Down syndrome and Alzheimer's disease.<sup>12,13</sup> Paralleling these diverse biological roles, basal concentrations of free  $\text{H}_2\text{S}$  are dynamic, interdependent with biological thiol concentrations, and sensitive to changes in redox homeostasis. As substrates in  $\text{H}_2\text{S}$  biosynthesis, fluctuations in Cys and Hcy concentrations can dramatically affect the kinetics of  $\text{H}_2\text{S}$  generation in enzymatic trans-sulfuration pathways.<sup>14</sup> Post-translational modification of Cys protein residues via oxidative S-sulfhydration to form hydrodisulfides (-SSH) or persulfides is also postulated to be an important  $\text{H}_2\text{S}$  storage mechanism, which modifies the antioxidant and signal transduction activity of  $\text{H}_2\text{S}$ .<sup>15–18</sup> Deconvoluting cellular  $\text{H}_2\text{S}$  generation, trans-

location, and metabolism steps is difficult, however, and chemists have been challenged to develop more accurate experimental methodologies for observing these processes. In particular, methods for the simultaneous detection and differentiation of  $\text{H}_2\text{S}$  and thiols would provide new insight into these multifaceted biological interactions.

Heightened research interest into the physiological properties of  $\text{H}_2\text{S}$  has led to the development of small molecule fluorescent probes which are able to more easily detect and quantify  $\text{H}_2\text{S}$ . Historical techniques for  $\text{H}_2\text{S}$  detection including gas chromatography, colorimetry, the methylene blue assay, and sulfur-selective electrodes all have limitations such as complex workups, slow response rates, and limited sensitivity.<sup>19–23</sup> One major challenge is differentiating between  $\text{H}_2\text{S}$  and thiols due to their similar modes of chemical reactivity. Recognizing and exploiting particular differences in  $\text{H}_2\text{S}$  and thiol reactivity, however, has been a key driver toward developing the rapidly emerging suite of small molecule fluorescent probes for  $\text{H}_2\text{S}$ . For example, although  $\text{H}_2\text{S}$  and thiols are both reducing agents,

Received: May 6, 2014

Accepted: June 17, 2014

Published: June 17, 2014

H<sub>2</sub>S reduces azide and nitro groups at a much faster rate than do thiols. Consequently, the selective H<sub>2</sub>S-mediated reduction of azide- and nitro-functionalized fluorophores to elicit a fluorescent response has been used as one strategy for H<sub>2</sub>S detection and imaging.<sup>24–39</sup> Other strategies, including the double-nucleophilic attack of H<sub>2</sub>S to release or change the photophysical properties of a bound fluorophore<sup>40–45</sup> and H<sub>2</sub>S-mediated metal sulfide precipitation from fluorophore-ligated metals,<sup>46–51</sup> have also been utilized for sulfide detection.

Several ratiometric probes have been developed for H<sub>2</sub>S, which have appealing characteristics compared with chemodosimeter probes.<sup>52–57</sup> The magnitude of fluorescence response with chemodosimeters is dependent on probe concentration, meaning that spatial variations in probe concentration caused by differential probe association with components of cellular milieu will reduce the accuracy and reliability of these platforms. Reaction-based ratiometric probes help to alleviate the problem of differential probe distribution by providing monitorable fluorescence emissions at two separate wavelengths, often corresponding to the unreacted probe and its subsequent reaction product. The ratio of these two fluorescence signals functions as an inherent self-calibration, decoupling the observed fluorescence response from probe concentration. A desirable extension of this strategy would be to monitor an additional species by fluorescence, thus allowing for the ratiometric determination of two different analytes simultaneously. To help unravel the intricacies of sulfur redox homeostasis, including H<sub>2</sub>S and thiol chemistry; a platform that could report on both H<sub>2</sub>S and thiols simultaneously would provide a way to differentiate between their respective concentrations, with long-term potential applications in diseases in which H<sub>2</sub>S and thiol concentrations are correlated.

As a proof of concept toward these long-term goals, we report herein the development and application of a platform for the ratiometric detection of H<sub>2</sub>S and Cys or Hcy based on a dual-fluorophore fragmentation strategy.

## ■ EXPERIMENTAL SECTION

**Materials and Methods.** Reagents were purchased from Sigma-Aldrich or Tokyo Chemical Industry (TCI) and used as received. Deuterated solvents were purchased from Cambridge Isotope Laboratories and used as received. Silica gel (SiliaFlash F60, Silicycle, 230–400 mesh) was used for column chromatography. <sup>1</sup>H and <sup>13</sup>C{<sup>1</sup>H} NMR spectra were recorded on a Varian INOVA 500 MHz NMR instrument. Chemical shifts are reported in parts per million relative to residual protic solvent resonances. UV–visible spectra were acquired on a Cary 100 spectrometer equipped with a Quantum Northwest TLC-42 dual cuvette temperature controller at 25.00 ± 0.05 °C. Fluorescence spectra were obtained on a Quanta Master 40 spectrofluorometer (Photon Technology International) equipped with a Quantum Northwest TLC-50 temperature controller at 25.0 ± 0.05 °C.

**Spectroscopic Materials and Methods.** Piperazine-*N,N'*-bis(2-ethanesulfonic acid) (PIPES, Aldrich) and potassium chloride (99.999%, Aldrich) were used to make buffered solutions (50 mM PIPES, 100 mM KCl, pH 7.4) in Millipore water. Anhydrous sodium hydrosulfide (NaHS) was purchased from Strem Chemicals and handled under nitrogen. Angeli's salt and DEA NONOate were purchased from Cayman and used to generate HNO and NO, respectively. Stock solutions of **NBD-Coum** in DMSO were prepared in an N<sub>2</sub>-filled glovebox

and stored at –25 °C until immediately prior to use. Stock solutions of L-cysteine, homocysteine, glutathione, serine, lysine, threonine, H<sub>2</sub>O<sub>2</sub>, Na<sub>2</sub>SO<sub>3</sub>, Na<sub>2</sub>SO<sub>4</sub>, and Na<sub>2</sub>S<sub>2</sub>O<sub>3</sub> in buffer and tyrosine in 0.1 M NaOH were freshly prepared in a glovebox. Stock solutions of NaHS in degassed buffer, and Angeli's salt and DEA NONOate in degassed 0.01 M NaOH, and L-cystine in degassed 1 M HCl were prepared under nitrogen immediately prior to use. All absorption and fluorescence measurements were made under anaerobic conditions, and cuvette solutions were prepared under an inert atmosphere in septum-sealed cuvettes obtained from Starna Scientific.

**General Procedure for Fluorescence and Selectivity Measurements.** A cuvette containing 3.0 mL of PIPES buffer (50 mM, 100 mM KCl, pH 7.4) and a septum cap was prepared in a glovebox. An **NBD-Coum** stock solution (15 μL, 1.0 mM) was added via syringe to the cuvette, and initial fluorescence spectra were recorded with excitation/emission at 400/405–600 nm and 475/485–650 nm. After addition of a NaHS stock solution (15 μL, 50 mM) via syringe and incubation at 25 °C for 15 min, fluorescence spectra were again recorded. For selectivity and ratiometric experiments, the emission maxima at 449 and 549 nm were compared.

**General Procedure for the Ratiometric Detection of H<sub>2</sub>S and Cysteine.** Stock solutions of NaHS (15 μL, 100 mM) and cysteine (15 μL, 100 mM) were combined and diluted with PIPES buffer (50 mM, 100 mM KCl, pH 7.4, 30 μL) to prepare a second stock solution containing 50 mM total sulfur content at a desired 1:1 H<sub>2</sub>S:Cys ratio. The fluorescence response of **NBD-Coum** was measured upon treatment with this second solution following the general procedure described above. The H<sub>2</sub>S:Cys stoichiometry in each experiment was controlled by varying the isolated H<sub>2</sub>S or Cys stock solution volumes used to prepare secondary stock solutions accordingly at the desired ratio.

**Procedure for Redox Comparisons.** A stock solution of L-cystine was prepared (25 mM) in 1 M HCl. Preliminary stock solutions of NaHS (15 μL, 100 mM) and cysteine (15 μL, 100 mM) were combined and diluted with PIPES buffer (50 mM, 100 mM KCl, pH 7.4, 30 μL) to prepare a second stock solution containing equimolar concentrations of NaSH and Cys (25 mM). A cuvette containing 3.0 mL of PIPES buffer (50 mM, 100 mM KCl, pH 7.4) and a septum cap was prepared under ambient atmosphere and purged with N<sub>2</sub>, air, or O<sub>2</sub> for 15 min. The cuvette was then charged with the NaHS/Cys (15 μL) and cystine (15 μL) stock solutions and incubated at 25 °C for 60 min to allow for equilibration of the sulfur pool. The cuvette was then injected with a **NBD-Coum** stock solution (15 μL, 1.0 mM), incubated an additional 15 min, and the fluorescence response of **NBD-Coum** at 449 and 549 nm was recorded. For the redox comparisons with NaOCl or TCEP, a cuvette containing 3.0 mL of PIPES buffer (50 mM, 100 mM KCl, pH 7.4) and a septum cap was prepared under ambient atmosphere. The cuvette was then charged with stock solutions of TCEP or NaOCl (15 μL, 50 mM), NaHS/Cys, and cystine and incubated at 25 °C for 60 min. The cuvette was injected with a **NBD-Coum** stock solution, incubated for 15 min, and the fluorescence response of **NBD-Coum** was measured.

**Synthesis of NBD-Coum.** A solution of 4-chloro-7-nitrobenzofurazan (60 mg, 0.32 mmol), 4-methylumbelliferone (42 mg, 0.24 mmol), and triethylamine (42 μL, 0.32 mmol) in DMF was stirred at room temperature for 1 h. The reaction mixture was then diluted with water and extracted into EtOAc.

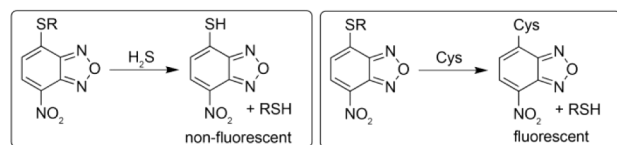
The organic phase was washed with brine and dried over  $\text{Na}_2\text{SO}_4$  to yield the crude product. Purification via column chromatography (hex:EtOAc gradient) afforded **NBD-Coum** as a pure orange solid (72 mg, 88%).  $^1\text{H}$  NMR (500 MHz, DMSO)  $\delta$  (ppm): 8.67 (d,  $J$  = 8.3 Hz, 1H), 7.98 (d,  $J$  = 8.7 Hz, 1H), 7.56 (d,  $J$  = 2.4 Hz, 1H), 7.44 (dd,  $J$  = 8.7, 2.4 Hz, 1H), 7.00 (d,  $J$  = 8.3 Hz, 1H), 6.46 (s, 1H), 2.48 (s, 3H).  $^{13}\text{C}\{^1\text{H}\}$  NMR (125 MHz, DMSO)  $\delta$  (ppm): 159.9, 156.1, 154.7, 153.4, 152.3, 145.9, 144.9, 135.6, 131.7, 128.3, 118.6, 117.2, 114.5, 112.3, 110.0, 18.7. HRMS ( $m/z$ ):  $[\text{M} + \text{H}]^+$  calcd for  $[\text{C}_{16}\text{H}_{10}\text{N}_3\text{O}_6]^+$  340.0565; found, 340.0570.

## RESULTS AND DISCUSSION

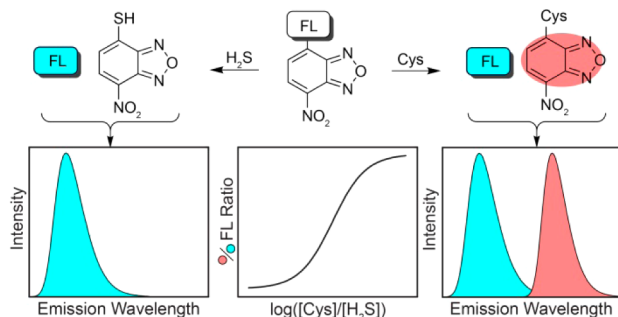
**Design and Synthesis of NBD-Coum.** Although several ratiometric fluorescent probes for  $\text{H}_2\text{S}$  have been reported, there are no examples of such constructs that report on the direct measurement of relative  $\text{H}_2\text{S}$  and thiol concentrations. To address this unmet need, we envisioned a reaction-based strategy that takes advantage of the nucleophilicity of  $\text{H}_2\text{S}$  and Cys/Hcy to cleave a covalent link between two bound fluorophores, nitrobenzofurazan (NBD) and coumarin. The key design principle is that reaction with sulfhydryl-containing nucleophiles results in fragmentation of NBD and coumarin. We demonstrated previously that  $\text{H}_2\text{S}$  and thiols readily undergo nucleophilic aromatic substitution ( $\text{S}_{\text{N}}\text{Ar}$ ) with electrophilic NBD derivatives to produce NBD-SH and NBD-SR compounds.<sup>58</sup> Upon reaction with Cys or Hcy, both coumarin and NBD-Cys/Hcy are fluorescent, whereas reaction with  $\text{H}_2\text{S}$  generates coumarin and nonfluorescent NBD-SH. Coumarin functions as an internal standard and allows for the ratiometric measurement of NBD-Cys/Hcy versus NBD-SH, and thus the Cys/Hcy to  $\text{H}_2\text{S}$  concentration ratios (Scheme 1).

**Scheme 1. General Strategy Employed in This Work for Generating a Ratiometric Response to  $\text{H}_2\text{S}$  and Cys/Hcy Levels**

### Previous work



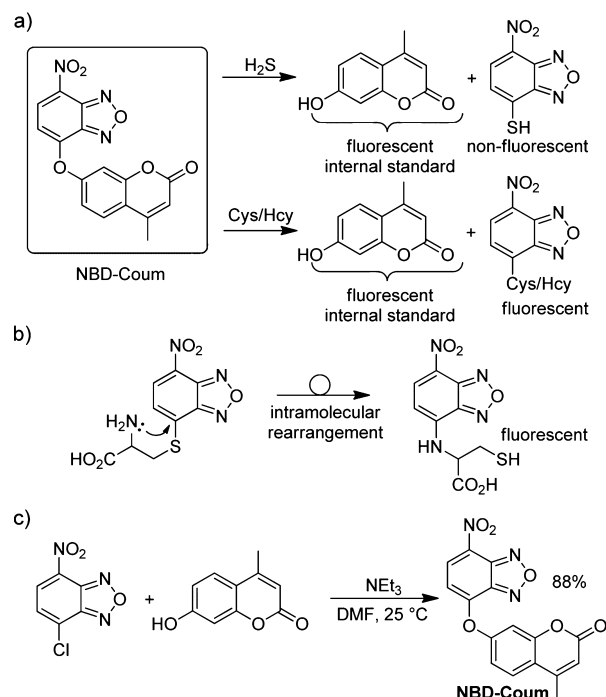
### This work



If each reaction product after reaction with  $\text{H}_2\text{S}$  or Cys provides distinct spectral features, we hypothesized that each could be monitored independently and used to determine relative concentrations of  $\text{H}_2\text{S}$  and Cys/Hcy in mixed-analyte environments. Although NBD-SH and NBD-SR are both nonfluorescent, NBD-adducts of Cys and Hcy undergo subsequent intermolecular rearrangement with adjacent amine

functionalities to form fluorescent amino-bound NBD-NHR compounds (Scheme 2a, b).<sup>59–61</sup> The second fluorophore

**Scheme 2. (a) Differential Reactivity of NBD-Coum with  $\text{H}_2\text{S}$  and Cys/Hcy Allows for the Ratio of  $\text{H}_2\text{S}$  and Cys/Hcy in a Sample to Be Determined, (b) Nonfluorescent S-bound NBD-Cys/Hcy Undergoes an Intramolecular Rearrangement to Form the Fluorescent N-Bound Adducts, and (c) Synthesis of NBD-Coum**



appended to the NBD scaffold through an ether linkage provides an additional fluorescent reporter that is liberated upon nucleophilic substitution. On the basis of this design, the coumarin fluorescence is directly proportional to the combined  $\text{H}_2\text{S}$  and Cys/Hcy concentrations in solution upon fragmentation of the probe, whereas the NBD component is proportional to the Cys/Hcy concentration exclusively, given that NBD-SH is nonfluorescent. Conveniently, the ratiometric probe **NBD-Coum** was prepared with good yield in one step from commercially available 4-chloro-7-nitrobenzofurazan (NBD-Cl) and 4-methylumbelliferone (coumarin) in DMF, using  $\text{NEt}_3$  as a base (Scheme 2c).<sup>62</sup>

**Spectroscopic Characteristics of NBD-Coum.** To evaluate the suitability of our design strategy and **NBD-Coum** as a platform for ratiometric determination of  $\text{H}_2\text{S}$  and Cys/Hcy levels, we first examined its reactivity with sulfhydryl-containing nucleophiles by UV-vis spectroscopy. Treatment of **NBD-Coum** (5  $\mu\text{M}$ ) with 50 equiv of NaHS, a common  $\text{H}_2\text{S}$  source, in PIPES buffer (50 mM, 100 mM KCl, pH 7.4) resulted in the rapid disappearance of **NBD-Coum** absorbance at 380 nm (<1 min) with concomitant appearance of two absorbances at 322 and 535 nm, corresponding to coumarin and NBD-SH, respectively. These results confirm that reaction of **NBD-Coum** with  $\text{H}_2\text{S}$  results in nearly instantaneous probe fragmentation into coumarin and NBD components. Treatment of **NBD-Coum** with either Cys or Hcy resulted in new absorbances centered at 475 nm, consistent with formation of amino-bound NBD.<sup>63</sup> By contrast, reaction of **NBD-Coum**



with either glutathione (GSH) or *N*-acetylcysteine (NAC), two thiols lacking the proximal amines required to undergo the intramolecular rearrangement, generated an absorbance at 425 nm, consistent with formation of NBD-SR adducts (Figure 1).

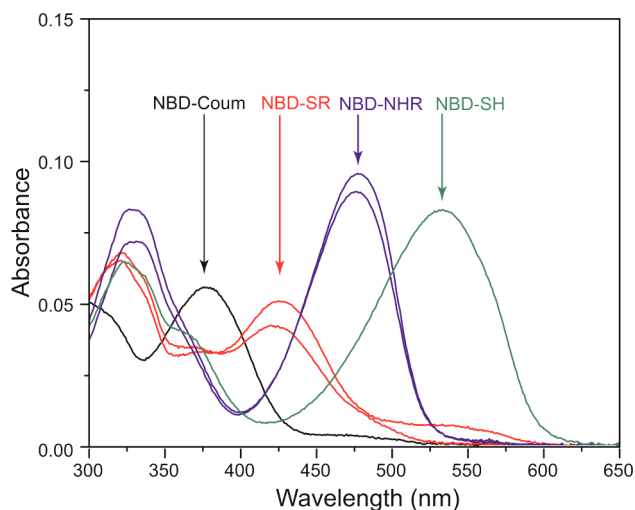


**Figure 1.** Comparison of the UV-vis spectra of **NBD-Coum** (5  $\mu$ M, black) and the HS-, RHN-, and RS-bound NBD products from reactions with 50 equiv of NaHS (250  $\mu$ M, green), Cys or Hcy (250  $\mu$ M, blue), and GSH or NAC (250  $\mu$ M, red) in PIPES buffer (50 mM, 100 mM KCl, pH 7.4) after incubation at 25  $^{\circ}$ C.

We next examined the reactivity of **NBD-Coum** with  $\text{H}_2\text{S}$  and Cys/Hcy by fluorescence spectroscopy to determine whether differentiable fluorescent products are produced in each case. In its unreacted state, **NBD-Coum** is nonfluorescent due to self-quenching of the bound coumarin and NBD fluorophores. Treatment of **NBD-Coum** with 50 equiv of NaHS resulted in ejection of the coumarin fluorophore and generation of a strong emission band centered at 449 nm. As established previously, NBD-SH is nonfluorescent due to the high acidity of the sulfhydryl proton and consequent deprotonation at pH 7.4.<sup>58</sup> By contrast to the reactivity observed with NaHS, reaction of **NBD-Coum** with Cys or Hcy generated two fluorescent products corresponding to coumarin and the *N*-bound Cys/Hcy NBD adducts. Excitation at 322 and 475 nm resulted in two discrete fluorescence signals centered at 449 and 549 nm corresponding to coumarin and NBD-Cys/Hcy, respectively. These results are again consistent with the dual-fluorophore fragmentation design, liberating coumarin upon reaction of **NBD-Coum** with either  $\text{H}_2\text{S}$  or Cys/Hcy, providing an internal standard for ratiometric differentiation. The resulting NBD product, however, is nonfluorescent from reaction with  $\text{H}_2\text{S}$  and fluorescent with Cys/Hcy reaction. The 100 nm separation between coumarin and NBD-Cys/Hcy fluorescence maxima allows for unambiguous measurement of each signal.

**Ratiometric Detection of  $\text{H}_2\text{S}$  and Cys.** To further validate our design strategy, we next investigated the dynamic range of the system by treating **NBD-Coum** (5  $\mu$ M) with mixed Cys: $\text{H}_2\text{S}$  solutions with stoichiometries ranging from 1:75 to 75:1, while keeping the total sulfur concentration constant in all samples (50 equiv). Under these experimental conditions, the two terminal data points represent 3.247  $\mu$ M in Cys: $\text{H}_2\text{S}$  and  $\text{H}_2\text{S}$ :Cys, respectively; however, lower analyte detection limits should be accessible using lower probe and/or

analyte concentrations. In each experiment, the fluorescence intensities at 449 nm (coumarin) and 549 nm (NBD-Cys) were measured.<sup>64</sup> As the  $[\text{Cys}]/[\text{H}_2\text{S}]$  ratio increases, more NBD-Cys is formed relative to NBD-SH, thus generating a stronger fluorescent signal at 549 nm. Consistent with our design hypothesis, the  $F_{549}/F_{449}$  ratio increased accordingly with higher  $[\text{Cys}]/[\text{H}_2\text{S}]$ . Furthermore, measurement of the ratio of the fluorescence intensities from coumarin and NBD-Cys generated a sigmoidal response ( $R^2 = 0.997$ ), which allows for the ratiometric determination of relative  $\text{H}_2\text{S}$  and Cys concentrations with a dynamic range of nearly 3 orders of magnitude (Figure 2).

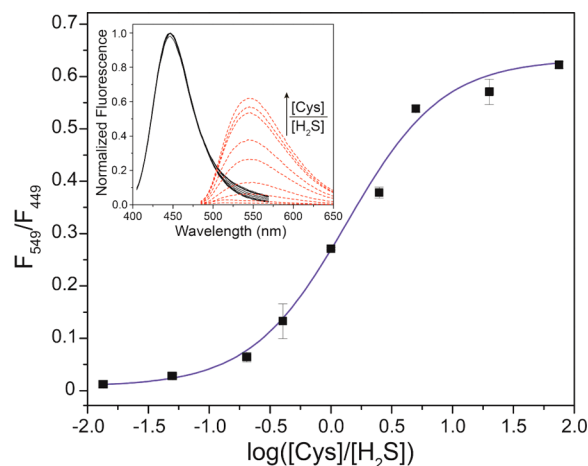


**Figure 2.** Ratiometric response ( $F_{549}/F_{449}$ ) of **NBD-Coum** to varying Cys: $\text{H}_2\text{S}$  stoichiometries (75:1, 20:1, 5:1, 2.5:1, 1:1, 1:2.5, 1:5, 1:20, and 1:75). Inset: Resultant fluorescence spectra from varying Cys: $\text{H}_2\text{S}$  ratios. Normalized coumarin fluorescence ( $\lambda_{\text{ex}} = 400$  nm,  $\lambda_{\text{em}} = 449$  nm) remains constant while NBD-Cys fluorescence ( $\lambda_{\text{ex}} = 475$  nm,  $\lambda_{\text{em}} = 549$  nm) increases with  $[\text{Cys}]/[\text{H}_2\text{S}]$ . Conditions: 5  $\mu$ M **NBD-Coum**, 250  $\mu$ M combined NaHS + Cys, PIPES buffer (50 mM, 100 mM KCl, pH 7.4). Data were acquired after 15 min incubation at 25  $^{\circ}$ C. Each data point represents the average of three trials. Error bars were calculated as standard error.

**Selectivity of **NBD-Coum**.** Having demonstrated the efficacy of the **NBD-Coum** platform in detecting different  $\text{H}_2\text{S}$ :Cys ratios, we next investigated the selectivity of the probe for  $\text{H}_2\text{S}$  and Cys/Hcy over other biologically relevant nucleophiles and reactive sulfur, oxygen, and nitrogen species (RSOs). **NBD-Coum** (5  $\mu$ M) was treated with 10 equiv of nucleophilic amino acids (Ser, Tyr, Lys, and Thr), oxidizing agents ( $\text{H}_2\text{O}_2$ ), sulfur anions ( $\text{SO}_3^{2-}$ ,  $\text{SO}_4^{2-}$ , and  $\text{S}_2\text{O}_3^{2-}$ ), and reactive nitrogen species (NO and HNO). In all cases, incubation for 15 min resulted in a negligible fluorescence response at both 449 and 549 nm (Figure 3). Treatment of **NBD-Coum** with GSH released the coumarin fluorophore and generated S-bound NBD-GSH, which was essentially non-fluorescent, and no turn-on at 549 nm was observed. Oxygen and nitrogen nucleophiles were insufficiently nucleophilic at physiological pH to react with **NBD-Coum**, which indicates that fragmentation of **NBD-Coum** into its respective NBD and coumarin components requires  $\text{S}_{\text{N}}\text{Ar}$  by stronger sulfhydryl-containing nucleophiles. Taken together, these selectivity studies highlight the selectivity of the **NBD-Coum** scaffold for differentiating between  $\text{H}_2\text{S}$  and Cys/Hcy. Although high levels of GSH would likely interfere with the ability of **NBD-Coum** to effectively differentiate  $\text{H}_2\text{S}$  and Cys/Hcy in many

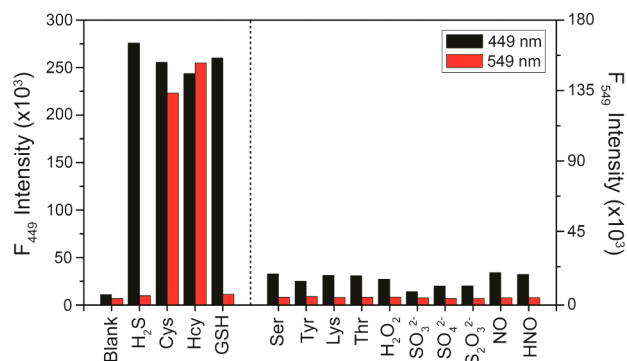


**Figure 3.** Selectivity profile of NBD-Coum toward nucleophilic amino acids and reactive sulfur, oxygen, and nitrogen species. From left to right: blank, NaHS, L-cysteine, DL-homocysteine, glutathione, L-serine, L-tyrosine, L-lysine, L-threonine,  $\text{H}_2\text{O}_2$ ,  $\text{Na}_2\text{SO}_3$ ,  $\text{Na}_2\text{SO}_4$ ,  $\text{Na}_2\text{S}_2\text{O}_3$ , DEA NONOate, and Angeli's salt. Conditions: 5  $\mu\text{M}$  NBD-Coum, 50  $\mu\text{M}$  RSONs, PIPES buffer (50 mM, 100 mM KCl, pH 7.4),  $\lambda_{\text{ex}}/\lambda_{\text{em}} = 400 \text{ nm}/449 \text{ and } 475 \text{ nm}/549$ . Data were acquired at 25  $^\circ\text{C}$  after 15 min incubation.

live-cell experiments, studies in blood plasma may still be accessible due to much lower concentrations of free GSH.

**Measurement of Redox Changes in Mixed Sulfur Pools.** Sulfur pools of  $\text{H}_2\text{S}$  and sulfhydryl-containing amino acids and peptides respond continuously to various levels of oxidative stress in biological systems by undergoing changes in their redox states. To simulate such changes, we investigated whether NBD-Coum could detect changes in oxidative stress levels in a simulated sulfur pool consisting of  $\text{H}_2\text{S}$  (125  $\mu\text{M}$ ), Cys (125  $\mu\text{M}$ ), and cystine (250  $\mu\text{M}$ ) (Figure 4). All

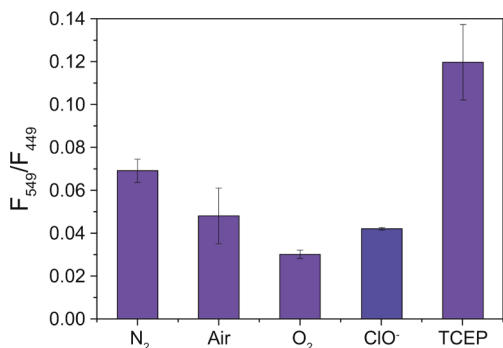


**Figure 4.** Response of the sulfur pool containing  $\text{H}_2\text{S}$ , Cys, and cystine to oxidative and reductive influences. Relative Cys: $\text{H}_2\text{S}$  ratios decrease under oxidative conditions and increase under reducing conditions. Conditions: The initial sulfur pool (125  $\mu\text{M}$   $\text{H}_2\text{S}$ , 125  $\mu\text{M}$  Cys, 250  $\mu\text{M}$  cystine) was incubated in PIPES buffer (50 mM, 100 mM KCl, pH 7.4) for 60 min at 25  $^\circ\text{C}$  under each redox condition and treated with 5  $\mu\text{M}$  NBD-Coum.

experiments were compared to a control case in which the sulfur species were combined in an  $\text{N}_2$ -purged cuvette. To increase the oxidative conditions, the sample was bubbled with either air or  $\text{O}_2$  or alternatively treated with NaOCl. Treatment of the sample with tris(2-carboxyethyl)phosphine (TCEP), a common reductant used to reduce disulfides, was used to mimic reductive conditions. In all cases of induced oxidative stress, the relative ratio of Cys/ $\text{H}_2\text{S}$  decreased, which is consistent with Cys oxidation. By contrast, under reductive conditions, the ratio of Cys/ $\text{H}_2\text{S}$  increased, which is consistent with TCEP-mediated reduction of cystine to Cys. Taken

together, these results demonstrate that NBD-Coum is able to effectively monitor changes in redox state in the sulfur pool.

## CONCLUSIONS

We have demonstrated the design and application of a platform to effectively measure  $\text{H}_2\text{S}$  and Cys/Hcy ratios using a dual-fluorophore fragmentation strategy. The mechanism of action relies not only on the differences in reactivity of  $\text{H}_2\text{S}$  and Cys/Hcy to provide differentiable reaction products with NBD-Coum but also in their similarity as potent nucleophiles capable of undergoing  $\text{S}_{\text{N}}\text{Ar}$  with the electrophilic scaffold. The strategy described here introduces a new class of compounds that could offer insights into thiol- $\text{H}_2\text{S}$  dynamics such as redox homeostasis or enzymatic metabolism.

## ASSOCIATED CONTENT

### Supporting Information

NMR spectra of NBD-Coum. This material is available free of charge via the Internet at <http://pubs.acs.org>.

## AUTHOR INFORMATION

### Corresponding Author

\*E-mail: [pluth@uoregon.edu](mailto:pluth@uoregon.edu). Tel: (541)346-7477. Fax: (541)346-4643.

### Notes

The authors declare no competing financial interest.

## ACKNOWLEDGMENTS

We thank Loveprit Singh for helpful discussions and assistance. This work was supported by the National Institute of General Medical Sciences (R00 GM092970) and funding from the University of Oregon. The NMR facilities at the University of Oregon are supported by NSF/ARRA CHE-0923589. The Biomolecular Mass Spectrometry Core of the Environmental Health Sciences Core Center at Oregon State University is supported, in part, by the NIEHS (P30ES000210) and the NIH.

## REFERENCES

- (1) Kazuho, A.; Kimura, H. *J. Neurosci.* **1996**, *16*, 1066–1071.
- (2) Kimura, H.; Nagai, Y.; Umemura, K.; Kimura, Y. *Antioxid. Redox. Signal.* **2005**, *7*, 795–803.
- (3) Ritter, J. M. *Br. J. Clin. Pharmacol.* **2010**, *69*, 573–575.
- (4) Wang, R. *Physiol. Rev.* **2012**, *92*, 791–896.
- (5) Wang, R. *Antioxid. Redox. Signal.* **2003**, *5*, 493–501.
- (6) Kimura, H. *Mol. Neurobiol.* **2002**, *26*, 13–19.
- (7) Yang, G.; Wu, L.; Wang, R. *FASEB J.* **2006**, *20*, 553–555.
- (8) Siebert, N.; Cantre, D.; Eipel, C.; Vollmar, B. *Am. J. Physiol.: Gastrointest. Liver Physiol.* **2008**, *295*, G1266–1273.
- (9) Jhee, K. H.; Kruger, W. D. *Antioxid. Redox. Signal.* **2005**, *7*, 813–822.
- (10) Stipanuk, M. H.; Beck, P. W. *Biochem. J.* **1982**, *206*, 267–277.
- (11) Shibuya, N.; Tanaka, M.; Yoshida, M.; Ogasawara, Y.; Togawa, T.; Ishii, K.; Kimura, H. *Antioxid. Redox. Signal.* **2009**, *11*, 703–714.
- (12) Ichinohe, A.; Kanaumi, T.; Takashima, S.; Enokido, Y.; Nagai, Y.; Kimura, H. *Biochem. Biophys. Res. Commun.* **2005**, *338*, 1547–1550.
- (13) Eto, K.; Asada, T.; Arima, K.; Makifuchi, T.; Kimura, H. *Biochem. Biophys. Res. Commun.* **2002**, *293*, 1485–1488.
- (14) Singh, S.; Padovani, D.; Leslie, R. A.; Chiku, T.; Banerjee, R. *J. Biol. Chem.* **2009**, *284*, 22457–22466.
- (15) Mustafa, A. K.; Gadalla, M. M.; Sen, N.; Kim, S.; Mu, W.; Gazi, S. K.; Barrow, R. K.; Yang, G.; Wang, R.; Snyder, S. H. *Sci. Signal.* **2009**, *2*, ra72.
- (16) Gadalla, M. M.; Snyder, S. H. *J. Neurochem.* **2010**, *113*, 14–26.

- (17) Predmore, B. L.; Lefer, D. J.; Gojon, G. *Antioxid. Redox. Signal.* **2012**, *17*, 119–140.
- (18) Ju, Y.; Zhang, W.; Pei, Y.; Yang, G. *Can. J. Physiol. Pharmacol.* **2013**, *91*, 8–14.
- (19) Wardencki, W. *J. Chromatogr. A* **1998**, *793*, 1–19.
- (20) Fogo, J. K.; Popowsky, M. *Anal. Chem.* **1949**, *21*, 732–734.
- (21) Doeller, J. E.; Isbell, T. S.; Benavides, G.; Koenitzer, J.; Patel, H.; Patel, R. P.; Lancaster, J. R., Jr; Darley-Usmar, V. M.; Kraus, D. W. *Anal. Biochem.* **2005**, *341*, 40–51.
- (22) M. F. Choi, M. *Analyst* **1998**, *123*, 1631–1634.
- (23) García-Calzada, M.; Marbán, G.; Fuertes, A. B. *Anal. Chim. Acta* **1999**, *380*, 39–45.
- (24) Lippert, A. R.; New, E. J.; Chang, C. J. *J. Am. Chem. Soc.* **2011**, *133*, 10078–10080.
- (25) Peng, H.; Cheng, Y.; Dai, C.; King, A. L.; Predmore, B. L.; Lefer, D. J.; Wang, B. *Angew. Chem., Int. Ed.* **2011**, *50*, 9672–9675.
- (26) Montoya, L. A.; Pluth, M. D. *Chem. Commun.* **2012**, *48*, 4767–4769.
- (27) Cao, X.; Lin, W.; Zheng, K.; He, L. *Chem. Commun.* **2012**, *48*, 10529–10531.
- (28) Hartman, M. C. T.; Dcona, M. M. *Analyst* **2012**, *137*, 4910–4912.
- (29) Chen, S.; Chen, Z.-J.; Ren, W.; Ai, H.-W. *J. Am. Chem. Soc.* **2012**, *134*, 9589–9592.
- (30) Das, S. K.; Lim, C. S.; Yang, S. Y.; Han, J. H.; Cho, B. R. *Chem. Commun.* **2012**, *48*, 8395–8397.
- (31) Zheng, K.; Lin, W.; Tan, L. *Org. Biomol. Chem.* **2012**, *10*, 9683–9688.
- (32) Wang, R.; Yu, F.; Chen, L.; Chen, H.; Wang, L.; Zhang, W. *Chem. Commun.* **2012**, *48*, 11757–11759.
- (33) Chen, B.; Lv, C.; Tang, X. *Anal. Bioanal. Chem.* **2012**, *404*, 1919–1923.
- (34) Bailey, T. S.; Pluth, M. D. *J. Am. Chem. Soc.* **2013**, *135*, 16697–16704.
- (35) Lin, V. S.; Lippert, A. R.; Chang, C. J. *Proc. Natl. Acad. Sci. U.S.A.* **2013**, *110*, 7131–7135.
- (36) Chen, B.; Li, W.; Lv, C.; Zhao, M.; Jin, H.; Jin, H.; Du, J.; Zhang, L.; Tang, X. *Analyst* **2013**, *138*, 946–951.
- (37) Sun, W.; Fan, J.; Hu, C.; Cao, J.; Zhang, H.; Xiong, X.; Wang, J.; Cui, S.; Sun, S.; Peng, X. *Chem. Commun.* **2013**, *49*, 3890–3892.
- (38) Zhou, G.; Wang, H.; Ma, Y.; Chen, X. *Tetrahedron* **2013**, *69*, 867–870.
- (39) Santos-Figueroa, L. E.; de la Torre, C.; El Sayed, S.; Sancenón, F.; Martínez-Máñez, R.; Costero, A. M.; Gil, S.; Parra, M. *Eur. J. Org. Chem.* **2014**, 1848–1854.
- (40) Liu, C.; Pan, J.; Li, S.; Zhao, Y.; Wu, L. Y.; Berkman, C. E.; Whorton, A. R.; Xian, M. *Angew. Chem., Int. Ed.* **2011**, *50*, 10327–10329.
- (41) Shen, X.; Pattillo, C. B.; Pardue, S.; Bir, S. C.; Wang, R.; Kevil, C. G. *Free Radical Biol. Med.* **2011**, *50*, 1021–1031.
- (42) Qian, Y.; Karpus, J.; Kabil, O.; Zhang, S.-Y.; Zhu, H.-L.; Banerjee, R.; Zhao, J.; He, C. *Nat. Commun.* **2011**, *2*, 495.
- (43) Liu, C.; Peng, B.; Li, S.; Park, C.-M.; Whorton, A. R.; Xian, M. *Org. Lett.* **2012**, *14*, 2184–2187.
- (44) Qian, Y.; Zhang, L.; Ding, S.; Deng, X.; He, C.; Zheng, X. E.; Zhu, H.-L.; Zhao, J. *Chem. Sci.* **2012**, *3*, 2920–2923.
- (45) Wei, C.; Zhu, Q.; Liu, W.; Chen, W.; Xi, Z.; Yi, L. *Org. Biomol. Chem.* **2014**, *12*, 479–485.
- (46) Sasakura, K.; Hanaoka, K.; Shibuya, N.; Mikami, Y.; Kimura, Y.; Komatsu, T.; Ueno, T.; Terai, T.; Kimura, H.; Nagano, T. *J. Am. Chem. Soc.* **2011**, *133*, 18003–18005.
- (47) Gu, X.; Liu, C.; Zhu, Y.-C.; Zhu, Y.-Z. *Tetrahedron Lett.* **2011**, *52*, 5000–5003.
- (48) Zhang, D.; Jin, W. *Spectrochim. Acta, Part A* **2012**, *90*, 35–39.
- (49) Hou, F.; Huang, L.; Xi, P.; Cheng, J.; Zhao, X.; Xie, G.; Shi, Y.; Cheng, F.; Yao, X.; Bai, D.; Zeng, Z. *Inorg. Chem.* **2012**, *51*, 2454–2460.
- (50) Qu, X.; Li, C.; Chen, H.; Mack, J.; Guo, Z.; Shen, Z. *Chem. Commun.* **2013**, *49*, 7510–7512.
- (51) Zhu, A.; Luo, Z.; Ding, C.; Li, B.; Zhou, S.; Wang, R.; Tian, Y. *Analyst* **2014**, *139*, 1945–1952.
- (52) Yu, F.; Li, P.; Song, P.; Wang, B.; Zhao, J.; Han, K. *Chem. Commun.* **2012**, *48*, 2852–2854.
- (53) Liu, J.; Sun, Y.-Q.; Zhang, J.; Yang, T.; Cao, J.; Zhang, L.; Guo, W. *Chem.—Eur. J.* **2013**, *19*, 4717–4722.
- (54) Bae, S. K.; Heo, C. H.; Choi, D. J.; Sen, D.; Joe, E. H.; Cho, B. R.; Kim, H. M. *J. Am. Chem. Soc.* **2013**, *135*, 9915–9923.
- (55) Wan, Q.; Song, Y.; Li, Z.; Gao, X.; Ma, H. *Chem. Commun.* **2013**, *49*, S02–S04.
- (56) Yu, C.; Li, X.; Zeng, F.; Zheng, F.; Wu, S. *Chem. Commun.* **2013**, *49*, 403–405.
- (57) Wu, M.-Y.; Li, K.; Hou, J.-T.; Huang, Z.; Yu, X.-Q. *Org. Biomol. Chem.* **2012**, *10*, 8342–8347.
- (58) Montoya, L. A.; Pearce, T. F.; Hansen, R. J.; Zakharov, L. N.; Pluth, M. D. *J. Org. Chem.* **2013**, *78*, 6550–6557.
- (59) Niu, L.-Y.; Guan, Y.-S.; Chen, Y.-Z.; Wu, L.-Z.; Tung, C.-H.; Yang, Q.-Z. *J. Am. Chem. Soc.* **2012**, *134*, 18928–18931.
- (60) Liu, J.; Sun, Y.-Q.; Huo, Y.; Zhang, H.; Wang, L.; Zhang, P.; Song, D.; Shi, Y.; Guo, W. *J. Am. Chem. Soc.* **2013**, *136*, 574–577.
- (61) Chen, Y.-H.; Tsai, J.-C.; Cheng, T.-H.; Yuan, S.-S.; Wang, Y.-M. *Biosens. Bioelectron.* **2014**, *56*, 117–123.
- (62) During the preparation of this manuscript, a similar structure was reported for H<sub>2</sub>S detection. Bae, J.; Choi, J.; Park, T. J.; Chang, S.-K. *Tetrahedron Lett.* **2014**, *55*, 1171–1174.
- (63) Ghosh, P. B.; Whitehouse, M. W. *Biochem. J.* **1968**, *108*, 155–156.
- (64) When excited at their respective  $\lambda_{\text{max}}$  values, coumarin has >15-fold stronger fluorescence intensity than NBD-Cys. To set the two baseline fluorescence intensities at the same order of magnitude, coumarin was excited at 400 nm.